Hindawi Publishing Corporation
EURASIP Journal on Wireless Communications and Networking
Volume 2007, Article ID 30684, 9 pages
doi:10.1155/2007/30684

Research Article

Joint Estimation of Mutual Coupling, Element Factor, and Phase Center in Antenna Arrays

Marc Mowlér,[1] Björn Lindmark,[1] Erik G. Larsson,[1,2] and Björn Ottersten[1]

[1] *ACCESS Linnaeus Center, School of Electrical Engineering, Royal Institute of Technology (KTH), 100 44 Stockholm, Sweden*
[2] *Department of Electrical Engineering (ISY), Linköping University, 58183 Linköping, Sweden*

Received 17 November 2006; Revised 20 June 2007; Accepted 1 August 2007

Recommended by Robert W. Heath Jr.

A novel method is proposed for estimation of the mutual coupling matrix of an antenna array. The method extends previous work by incorporating an unknown phase center and the element factor (antenna radiation pattern) in the model, and treating them as nuisance parameters during the estimation of coupling. To facilitate this, a parametrization of the element factor based on a truncated Fourier series is proposed. The performance of the proposed estimator is illustrated and compared to other methods using data from simulations and measurements, respectively. The Cramér-Rao bound (CRB) for the estimation problem is derived and used to analyze how the required amount of measurement data increases when introducing additional degrees of freedom in the element factor model. We find that the penalty in SNR is 2.5 dB when introducing a model with two degrees of freedom relative to having zero degrees of freedom. Finally, the tradeoff between the number of degrees of freedom and the accuracy of the estimate is studied. A linear array is treated in more detail and the analysis provides a specific design tradeoff.

1. INTRODUCTION

Adaptive antenna arrays in mobile communication systems promise significantly improved performance [1–3]. However, practical limitations in the antenna arrays, for instance, interelement coupling, are not always considered. The array is commonly assumed ideal which means that the radiation patterns for the individual array elements are modelled as isotropic or omnidirectional with a far-field phase corresponding to the geometrical location. Unfortunately, this is not true in practice which leads to reduced performance as reported by [4–6]. One of the major contributors to the nonideal behavior is the mutual coupling between the antenna elements of the array [7, 8] and the result is a reduced performance [9, 10].

To model the mutual coupling, a matrix representation has been proposed whose inverse may be used to compensate the received data in order to extract the true signal [5]. For basic antenna types and array configurations, the coupling matrix can be obtained from electromagnetic calculations. Alternatively, calibration measurement data can be collected and the coupling matrix may be extracted from the data [11–13]. In [14], compensation with a coupling matrix was found superior to using dummy columns in the case of a 4-column dual polarized array. One difficulty that arises when estimating the coupling matrix from measurements is that other parameters such as the element factor and the phase center of the antenna array need to be estimated. These have been reported to influence the coupling matrix estimate [14].

Our work extends previous work [5, 11–14] by treating the radiation pattern and the array phase center as unknowns during the coupling estimation. We obtain a robust and versatile *joint* method for estimation of the coupling matrix, the element factor, and the phase center. The proposed method does not require the user to provide any a priori knowledge of the location of the array center or about the individual antenna elements.

The performance of the proposed joint estimator is compared via simulations of an 8-element antenna array to a previous method developed by the authors [13]. In addition, we illustrate the estimation performance based on actual measurements on an 8-element antenna array. Furthermore, a CRB analysis is presented which can be used as a performance benchmark. Finally, a tradeoff between the complexity of the model and the performance of the estimator is examined for an 8-element antenna array with element factor $\mathbf{E}_{\text{true}} = \cos(2\theta)$.

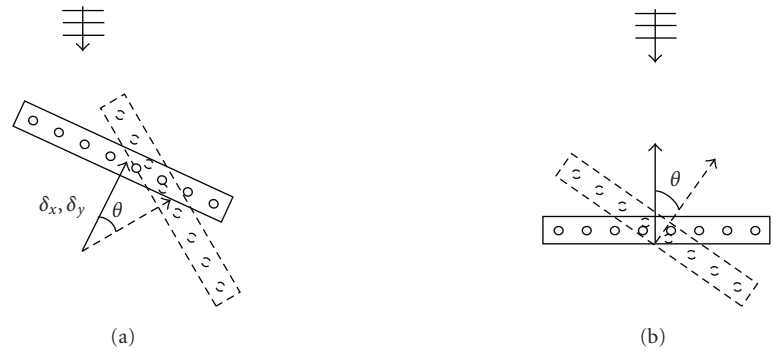

Figure 1: Schematic drawing of the antenna array with (a) and without (b) the displacement of the phase center relative to the origin of the coordinate system. Rotating the antenna array (solid) an angle θ gives a relative change (dashed) that depends on the distance to the origin (δ_x, δ_y).

2. DATA MODEL AND PROBLEM FORMULATION

Consider a uniform linear antenna array with M elements having an interelement spacing of d. A narrowband signal, $s(t)$, is emitted by a point source with direction-of-arrival θ relative to the broadside of the receiving array. The data collected by the array with true array response $\widetilde{a}(\theta)$ is [5, 14]

$$x = \widetilde{\mathbf{a}}(\theta)s(t) + \mathbf{w}, \quad \mathbf{x} \in \mathbb{C}^{M\times 1}. \tag{1}$$

We model $\widetilde{a}(\theta)$ as follows:

$$\widetilde{\mathbf{a}}(\theta) \simeq \mathbf{C}\mathbf{a}(\theta)e^{jk(\delta_x\cos\theta+\delta_y\sin\theta)}f(\theta), \quad \widetilde{\mathbf{a}} \in \mathbb{C}^{M\times 1}, \tag{2}$$

where the following conditions hold.

(i) $\widetilde{\mathbf{a}}(\theta)$ is the true radiation pattern in the far-field including mutual coupling, edge effects, and mechanical errors. $\widetilde{\mathbf{a}}(\theta)$ is modelled as suggested by (2).

(ii) $\mathbf{C}$ is the $M \times M$ coupling matrix. This matrix is complex-valued and unstructured. The main focus of this paper is to estimate $\mathbf{C}$.

(iii) $\{\delta_x, \delta_y\}$ is the array phase center. Figure 1 illustrates how the displacement of the antenna array is modelled by $\delta_x\hat{x} + \delta_y\hat{y}$ from the origin. The proposed approach also estimates $\{\delta_x, \delta_y\}$. Note that $\{\delta_x, \delta_y\}$ is not included in the models used in [5, 14].

(iv) $f(\theta) \geq 0$ is the element factor (antenna radiation pattern describing the real-valued amplitude of the electric field pattern) in direction θ without mutual coupling and describes the amount of radiation from the individual antenna elements of the array in different directions θ. $f(\theta)$ is real-valued and includes no direction-dependent phase shift [7]. The proposed estimator also estimates $f(\theta)$. Note that $f(\theta)$ was not included in the models used in [5, 14]. All antenna elements are implicitly assumed to have equal radiation patterns when not in an array configuration, that is, $f(\theta)$ is the same for all M elements. When the elements are placed in an array, the radiation patterns of each element are not the same due to the mutual coupling. However, $f(\theta)$ is allowed to be nonisotropic, which is also the case in practice.

(v) $\mathbf{a}(\theta)$ is a Vandermonde vector whose mth element is

$$a_m(\theta) = e^{jkd\sin\theta(m-M/2-1/2)}. \tag{3}$$

(vi) d is the distance between the antenna elements.

(vii) k is the wave number.

(viii) w is i.i.d complex Gaussian noise with zero-mean and variance σ^2 per element.

Based on calibration data, when a signal, $s(t) = 1$, is transmitted from N known direction-of-arrivals[1] $\{\theta_1, \ldots, \theta_N\}$, we collect one data vector $\mathbf{x}_n$ of measurements for each angle θ_n. The measurements are arranged in a matrix, $\mathbf{X} = [\mathbf{x}_1 \ \cdots \ \mathbf{x}_N]$, as follows:

$$\begin{aligned}
\mathbf{X} &= \mathbf{C}\mathbf{A}\mathbf{D}(\delta_x, \delta_y)\mathbf{E}(f(\theta)) + \mathbf{W},\\
\mathbf{A} &= [\mathbf{a}(\theta_1) \ \cdots \ \mathbf{a}(\theta_N)],\\
\mathbf{E}(f(\theta)) &= \operatorname{diag}\{f(\theta_1), \ldots, f(\theta_N)\},\\
\mathbf{D}(\delta_x, \delta_y) &= \operatorname{diag}\{e^{jk(\delta_x\cos\theta_1+\delta_y\sin\theta_1)}, \ldots, e^{jk(\delta_x\cos\theta_N+\delta_y\sin\theta_N)}\}.
\end{aligned} \tag{4}$$

The matrix $\mathbf{W}$ represents measurement noise, which is assumed to be i.i.d zero-mean complex Gaussian with variance σ^2 per element. In this paper, we propose a method to estimate $\mathbf{C}$ when δ_x, δ_y, and $f(\theta)$ are *unknown*.

One of the novel aspects of the proposed estimator is the inclusion of the element factor, $f(\theta)$, as a jointly unknown parameter during the estimation of the coupling matrix, $\mathbf{C}$. This requires a parametrization that provides a flexible and mathematically appealing representation of an a priori unknown element factor. We have chosen to model $f(\theta)$ as a linear combination of sinusoidal basis functions according to

$$f(\theta) = \sum_{k=1}^{K} \alpha_k \cos(k-1)\theta, \quad |\theta| < \frac{\pi}{2}, \tag{5}$$

[1] The orientation of the array is assumed to be perfectly known, while the exact position of the phase center is typically unknown during the antenna calibration.

where K is a known (small) integer, and α are unknown and real-valued constants. Equation (5) is effectively equivalent to a truncated Fourier series where the coefficients are to be estimated. Even though the chosen parametrization may assume negative values, it is introduced to allow the element factor, **E**, to assume arbitrary shapes that can match the true pattern of the measured antenna array. This can increase the accuracy in the estimate of **C** compared to only assuming an omnidirectional element factor that would correspond to $E = I$.

Other alternative parameterizations of $f(\theta)$ exist as well. A piecewise constant function of θ is one example. The proposed parametrization, on the other hand, is particularly attractive since the basis functions are orthogonal and at the same time smooth. Additionally, the unknown coefficients, α_k, enter the model linearly. Based on (5), the element factor can be expressed as

$$\begin{aligned}\mathbf{E} &= \sum_{k=1}^{K} \alpha_k \mathbf{Q}_k,\\ \boldsymbol{\alpha} &= \begin{bmatrix}\alpha_1 & \cdots & \alpha_K\end{bmatrix}^T,\\ \mathbf{Q}_k &= \operatorname{diag}\{\cos(k-1)\theta_1, \ldots, \cos(k-1)\theta_N\}.\end{aligned} \tag{6}$$

The coefficients, $\boldsymbol{\alpha}$, will be jointly estimated together with the coupling matrix and phase center by the estimator proposed in this paper.

3. THE PROPOSED ESTIMATOR

We propose to estimate **C**, $\boldsymbol{\alpha}$, δ_x, and δ_y from **X** by using a least-squares criterion[2] on the data model expressed in (4) according to

$$\min_{\mathbf{C},\boldsymbol{\alpha},\delta_x,\delta_y} ||\mathbf{X} - \mathbf{CAD}(\delta_x,\delta_y)\mathbf{E}(\boldsymbol{\alpha})||_F^2. \tag{7}$$

Under the assumption of Gaussian noise, (7) is the maximum-likelihood estimator. The values of $\mathbf{C}, \boldsymbol{\alpha}, \delta_x, \delta_y$ that minimize the Frobenius norm in (7) are found using an iterative approach. The coupling matrix, the matrix **C** is first expressed as if the other parameters were known followed by a minimization over the $\boldsymbol{\alpha}$ parameters while keeping **C** and $\{\delta_x, \delta_y\}$ fixed. A second minimization is made over $\{\delta_x, \delta_y\}$ with **C** and $\boldsymbol{\alpha}$ treated as constants after which the algorithm loops back to minimize over $\boldsymbol{\alpha}$ again. The steps of the estimator are as follows:

(1) minimize (7) with respect to the coupling matrix, **C**, while the phase center, $\{\delta_x, \delta_y\}$, and the element factor representation, $\boldsymbol{\alpha}$, are fixed. This is done using the pseudoinverse approach expressed by [4]

$$\hat{\mathbf{C}} = \mathbf{X}(\mathbf{ADE})^H\left[\mathbf{ADE}(\mathbf{ADE})^H\right]^{-1}; \tag{8}$$

(2) minimize (7) with respect to $\boldsymbol{\alpha}$ while **C**, δ_x, and δ_y are fixed. In this step, the value of **C** found in the previous step is used as the assumed constant value for the coupling matrix; the minimization over $\boldsymbol{\alpha}$ is then performed using the following manipulations: first, rearrange the measurement matrix, **X**, and the expression (4) in vectorized form as

$$\begin{aligned}\mathbf{x} &= \begin{bmatrix}\operatorname{vec}\{\operatorname{Re}\{\mathbf{X}\}\}\\ \operatorname{vec}\{\operatorname{Im}\{\mathbf{X}\}\}\end{bmatrix},\\ \mathbf{Y} &= \begin{bmatrix}\operatorname{vec}\{\operatorname{Re}\{\mathbf{CAD}Q_1\}\} & \cdots & \operatorname{vec}\{\operatorname{Re}\{\mathbf{CAD}Q_K\}\}\\ \operatorname{vec}\{\operatorname{Im}\{\mathbf{CAD}Q_1\}\} & \cdots & \operatorname{vec}\{\operatorname{Im}\{\mathbf{CAD}Q_K\}\}\end{bmatrix};\end{aligned} \tag{9}$$

the least-squares criterion used is then expressed as

$$\min_{\boldsymbol{\alpha}} ||\mathbf{x} - \mathbf{Y}\alpha||_F^2 \tag{10}$$

with the solution

$$\hat{\boldsymbol{\alpha}} = \left(\mathbf{Y}^T\mathbf{Y}\right)^{-1}\mathbf{Y}^T\mathbf{x}, \tag{11}$$

which gives the minimizing $\boldsymbol{\alpha}$ parameters;

(3) minimize (7) with respect to δ_x and δ_y while keeping **C** and $\boldsymbol{\alpha}$ fixed. Using the $\boldsymbol{\alpha}$ parameters found in the previous step, **C**, is expressed again according to (8). Assuming the other parameters to be constant, a two-dimensional gradient search is conducted to find the minimizing $\{\delta_x, \delta_y\}$ of (7). Steps 1–3 are iterated until $\|\mathbf{X} - \hat{\mathbf{C}}\mathbf{A}\hat{\mathbf{D}}\hat{\mathbf{E}}\|_F^2$ is within a certain tolerance level.

To provide the algorithm with an initial estimate, in the first iteration, we take $\mathbf{D} = \mathbf{I}$ and $\boldsymbol{\alpha} = [0, 1, 0, \ldots, 0]^T$, which corresponds to the element factor $f(\theta) = \cos\theta$ that was used in [13]. The initialization of the algorithm could of course be done in many different ways and this may affect its performance. The choice considered here can be seen as a refinement of the algorithm previously proposed in [13].

Typically, about 5 iterations of the algorithm are required to reach a local optimum depending on the given tolerance level. Convergence to the global optimum can not be assured; however, the algorithm will converge since the cost function (7) is nonincreasing in each iteration. The topic has been addressed in previous conference papers [13].

4. CRAMÉR-RAO BOUND ANALYSIS

The parameter K, corresponding to the number of terms used in the truncated Fourier series representation of the element factor, is key to the proposed estimator. This value will affect the accuracy of the estimator. Increasing the value will give a better match between the true element factor and the assumed model. At the same time, it will increase the complexity of the model and complicate the estimation. Another aspect is the fact that increasing the value K towards infinity may not be the best way of tuning the algorithm if the true value is much less. This would force the estimator to use a model far more complicated than needed, leading to estimation of additional parameters. Even though the parameters would be close to zero, the performance of the estimator is still affected as indicated by the CRB analysis in this

[2] The minimum of this cost function is not unique, see Section 4 for a discussion of this.

section. On the other hand, a smaller number of parameters may give insufficient flexibility to the algorithm and force it into a nonoptimal result.

To compensate for the affected performance associated with a large value of K, the number of measurements N of x_n can be used as well as a higher signal-to-noise ratio (SNR). Let us now study the tradeoff between these three parameters by quantifying how the choice of K relates to N and the SNR ($1/\sigma^2$). The Cramér-Rao bound (CRB) for the estimation problem in (7) is derived and will provide a lower bound on the variance of the unknown parameters [15–17]. All the elements of $\mathbf{C}$ are considered to be unknown complex-valued parameters and therefore separated with respect to real and imaginary parts with C_{ij}^R denoting the real part of the element in the ith row and jth column, and C_{ij}^I denoting the corresponding imaginary part. All the $2M^2 + 2 + K$ real-valued unknown parameters of (4) are collected into the vector

$$\boldsymbol{\xi} = \left[C_{11}^R \cdots C_{1M}^R \cdots C_{MM}^R \cdots C_{ij}^I \;\; \delta_x \;\; \delta_y \;\; \alpha_1 \;\cdots\; \alpha_K\right]^T. \tag{12}$$

The CRB for the estimate of $\boldsymbol{\xi}$ is expressed by [15]

$$[\text{CRB}] = \left[\mathbf{I}_{\text{Fisher}}\right]^{-1}, \tag{13}$$

where $\mathbf{I}_{\text{Fisher}}$ is the Fisher information matrix given by

$$\left[\mathbf{I}_{\text{Fisher}}\right]_{ij} = \frac{2}{\sigma^2}\text{Re}\left\{\frac{\partial \boldsymbol{\mu}^H}{\partial \xi_i}\frac{\partial \boldsymbol{\mu}}{\partial \xi_j}\right\}, \tag{14}$$

where $\boldsymbol{\mu}$ is the expected value of $\mathbf{x}$ in (9). The problem (7) is unidentifiable as presented. The scaling ambiguity present between $\mathbf{C}$ and $\boldsymbol{\alpha}$ is solved by enforcing a constraint on the problem. Here, we choose to constrain $\|\mathbf{C}\|_F^2 = M$ as opposed to other possibilities such as $\alpha_1 = 1$ or $C_{11}^R = 1$. The latter favors particular elements of $\mathbf{C}$ or α by forcing these to be nonzero. This is undesirable and consequently ruled out. This constraint was also implemented as a normalization in the estimator presented in the previous section, while not mentioned there explicitly.

The CRB under parametric constraints is found by following the results derived in [18]. The constraint is expressed as

$$g(\boldsymbol{\xi}) = \|\mathbf{C}\|_F^2 - M = \mathbf{Tr}\{\mathbf{C}^H\mathbf{C}\} - M = 0. \tag{15}$$

Defining

$$\left[\mathbf{G}(\boldsymbol{\xi})\right]_l = \frac{\partial g(\boldsymbol{\xi})}{\partial \xi_l} = \begin{cases} 2\text{Re}\{c_{ij}\} & \text{if } \xi_l = \text{Re}\{c_{ij}\}, \\ 2\text{Im}\{c_{ij}\} & \text{if } \xi_l = \text{Im}\{c_{ij}\}, \\ 0 & \text{otherwise,} \end{cases} \tag{16}$$

the constrained CRB is given by [18]

$$[\text{CRB}] = \mathbf{U}\left(\mathbf{U}^T\mathbf{I}_{\text{Fisher}}\,\mathbf{U}\right)^{-1}\mathbf{U}^T, \tag{17}$$

where $\mathbf{U}$ is implicitly defined via $\mathbf{G}(\boldsymbol{\xi})\mathbf{U} = 0$. Note that the CRB is proportional to σ^2, that is, the estimation accuracy is inversely proportional to the SNR.

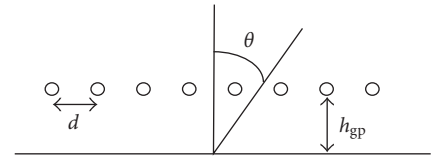

Figure 2: Schematic overview of the antenna array consisting of dipoles over an infinite ground plane. The distance from the ground plane is h_{gp} and the spacing between the elements is d. The angle from the normal to the antenna axis is denoted by θ.

5. RESULTS

5.1. Dipole array example

First, let us consider the case of an 8-element dipole array over a ground plane, see Figure 2. In the absence of mutual coupling, each element has the true radiation pattern

$$E_{\text{true}} = \sin(kh_{gp}\cos\theta), \tag{18}$$

where k is the wave number and h_{gp} is the distance to the ground plane. Using known expressions for mutual coupling between dipoles [7], it is straightforward to calculate the embedded element patterns. Figures 3(a) and 3(b) show the radiation pattern for a single element and an 8-element array with mutual coupling for $h_{gp} = 3\lambda/8$. The interelement spacing is $d = \lambda/2$ and the true $\{\delta_x, \delta_y\}$ are $\{0, 0\}$.

We now compare our proposed method using a truncated Fourier series expansion of the element factor, see (5), to results obtained by using a cosine-shaped ($E = \cos^n\theta$) element pattern assumption as in [13]. In our proposed method, the algorithm described in Section 3 is used to estimate $\mathbf{C}$, $\{\alpha_1, \alpha_2, \alpha_3\}$, and $\{\delta_x, \delta_y\}$, which corresponds to choosing $K = 3$ in the model for the element factor as expressed in (5). Similarly, the parameter n in the expression $E = \cos^n\theta$ is optimized as part of the procedure when using the method of [13]. In both cases, we make a starting assumption that $\{\delta_x, \delta_y\} = \{0, 0\}$, which is also the true value for this case.

With *no* compensation, the uncompensated radiation pattern is represented in Figure 3(b). *With* compensation, where a cosine-shaped element pattern ($E = \cos^n\theta$) is assumed, the resulting radiation pattern is displayed in Figure 3(c). The unknown values in addition to the mutual coupling matrix were estimated to $\hat{n} = 0.5$ and $\{\hat{\delta}_x, \hat{\delta}_y\} = \{0, 0\}$, and the performance is significantly improved over the uncompensated case. By allowing the model for the element factor to follow a truncated Fourier series ($K = 3$) according to our method, the performance of the mutual coupling matrix estimate is improved even more resulting in the graph of Figure 3(d). For this case, our method estimated the values for the auxiliary unknown parameters to be $\hat{\boldsymbol{\alpha}} = [-1.1 \;\; 3.1 \;\; -1.1]^T$ and $\{\hat{\delta}_x, \hat{\delta}_y\} = \{0, 0\}$. The result also agrees well with the true (ideal) radiation pattern when the mutual coupling is neglected as presented in Figure 3(a).

The phase error for the cases of uncompensated and compensated phase diagrams are presented in Figure 4. The top graph represents the uncompensated case, while the

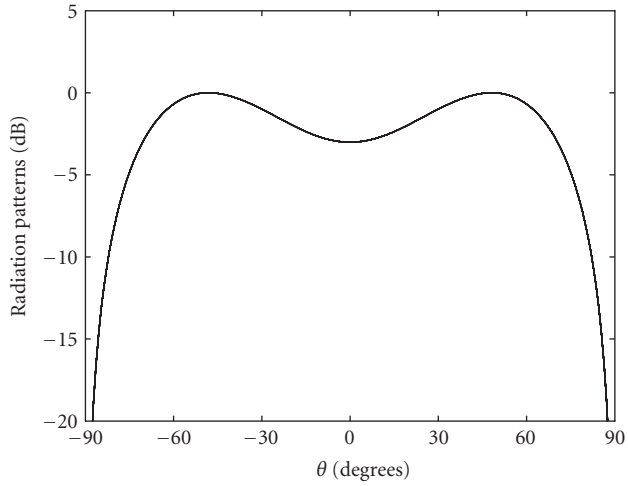

(a) *True* radiation patterns for a single element; $f(\theta)$

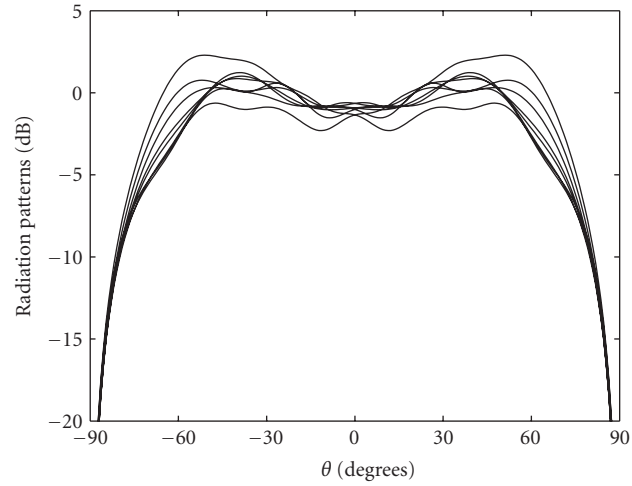

(b) *Uncompensated* radiation patterns with mutual coupling; $\mathbf{x}_1 \cdots \mathbf{x}_M$

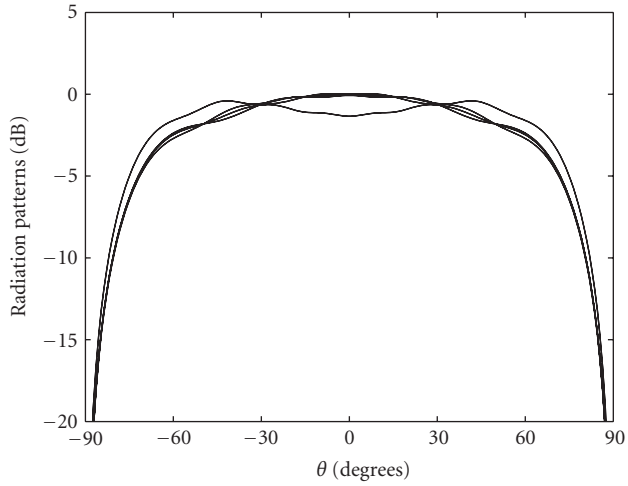

(c) Radiation patterns obtained from *compensated* data using a $\mathbf{C}$ matrix estimated via $\mathbf{E} = \cos^n\theta$ as the parametrization of the element factor [13]; $\mathbf{C}_{\cos}^{-1}\mathbf{x}_1 \cdots \mathbf{C}_{\cos}^{-1}\mathbf{x}_M$

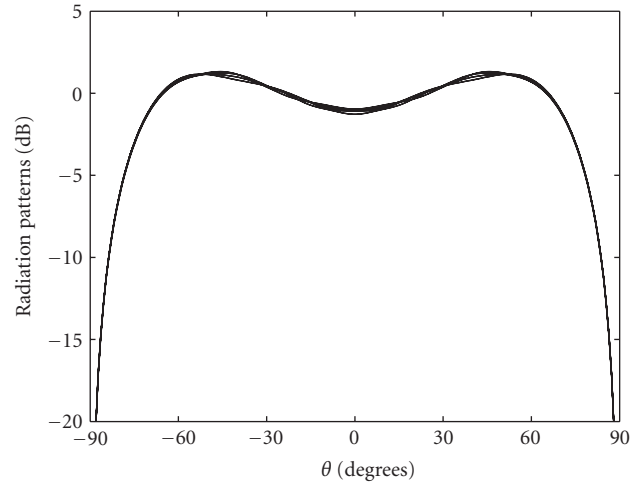

(d) *Compensated* radiation patterns using our method with $K = 3$; $\mathbf{C}^{-1}\mathbf{x}_1 \cdots \mathbf{C}^{-1}\mathbf{x}_M$

FIGURE 3: Compensation for mutual coupling for an array of 8 dipoles placed $h_{gp} = 3\lambda/8$ over a ground plane.

middle and bottom graphs represent compensated cases with a cosine-shaped and the truncated Fourier series parameterizations of the element factors, respectively. This also verifies that our method with $K = 3$ improves the result over constraining the element factor to be cosine-shaped ($E = \cos^n\theta$) as was proposed in previous work [13].

5.2. CRB for dipole array example

The CRB as a function of K (i.e., the order of the parametrization of $f(\theta)$) for an 8-element array of dipoles over ground plane is presented in Figure 5. When generating this figure, we used the theoretical models of [7] for the coupling between antenna elements with inter-element spacing $d = \lambda/2$. The true data used are based on a scenario when $K = 1$, $\mathbf{D} = \mathbf{I}$, and $\mathbf{E} = \mathbf{I}$. The SNR was 0 dB ($\sigma^2 = 1$). The four curves show

(i) $\text{CRB}_C = \text{Tr}\{\{\mathbf{U}_C(\mathbf{U}_C^T\mathbf{I}_C\mathbf{U}_C)^{-1}\mathbf{U}_C^T\}_C\}$, the CRB of $\mathbf{C}$ when both $\mathbf{D}$ and $\mathbf{E}$ are known;

(ii) $\text{CRB}_{CD} = \text{Tr}\{\{\mathbf{U}_{CD}(\mathbf{U}_{CD}^T\mathbf{I}_{CD}\mathbf{U}_{CD})^{-1}\mathbf{U}_{CD}^T\}_C\}$, the CRB of $\mathbf{C}$ when $\mathbf{D}$ is unknown and $\mathbf{E}$ is known;

(iii) $\text{CRB}_{CE} = \text{Tr}\{\{\mathbf{U}_{CE}(\mathbf{U}_{CE}^T\mathbf{I}_{CE}\mathbf{U}_{CE})^{-1}\mathbf{U}_{CE}^T\}_C\}$, the CRB of $\mathbf{C}$ when $\mathbf{D}$ is known and $\mathbf{E}$ is unknown;

(iv) $\text{CRB}_{CDE} = \text{Tr}\{\{\mathbf{U}_{CDE}(\mathbf{U}_{CDE}^T\mathbf{I}_{CDE}\mathbf{U}_{CDE})^{-1}\mathbf{U}_{CDE}^T\}_C\}$, the CRB of $\mathbf{C}$ when $\mathbf{D}$ and $\mathbf{E}$ are unknown.

The results in Figure 5 quantify the increase in achievable estimation performance for the elements of $\mathbf{C}$ when increasing the number of nuisance parameters in the model. In particular, we see that the estimation problem becomes more difficult when more $\boldsymbol{\alpha}$ parameters are introduced in the model. For example, it is more difficult to estimate the coupling matrix $\mathbf{C}$ when the phase center δ_x, δ_y, is unknown. However,

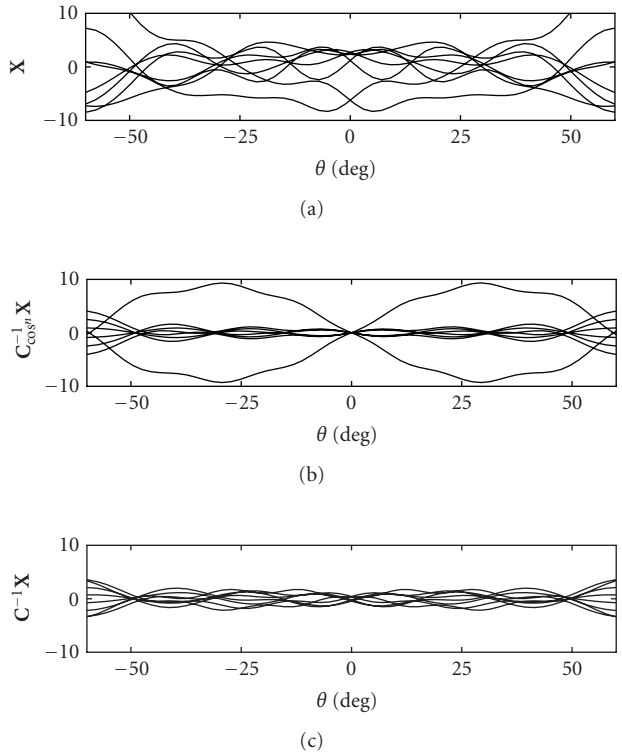

Figure 4: Uncompensated (a) and compensated (b, c) phase diagrams with $\mathbf{E} = \cos^n\theta$ and $\mathbf{E} = \sum \alpha_k \mathbf{Q}_k$, respectively. The true element factor is $\mathbf{E}_{\text{true}} = \sin(2\pi(3/8)\cos\theta)$, which corresponds to $h_{gp} = 3\lambda/8$.

for $K \geq 3$, the difficulty of identifying $\boldsymbol{\alpha}$ dominates over the problem of estimating the phase center. Since the CRB is proportional to σ^2, the increase in emitter power (i.e., SNR) required to maintain a given performance when the model is increased with more unknowns can be seen in the figure.

In Figure 6, the CRB as a function of K and N is studied. From this figure, we can directly read out how much higher emitter power (or equivalently, lower σ^2) is required to be able to maintain the same estimation performance for $\mathbf{C}$ when K or N vary. For example, if fixing $N = 100$, say, then going from $K = 1$ to $K = 2$ requires 1 dB additional SNR. Going from $K = 2$ to $K = 3$ requires an increase of the SNR level by 1.5 dB. However, going from $K = 3$ to 4 requires 10 dB extra SNR. Thus, $K = 3$ appears to be a reasonable choice. In practice, it is difficult to handle more than $K = 3$ for the element factor in this case.

In Figure 6, we observe that in the limit when the number of angles reaches $N = 15$, the problem becomes unidentifiable. This is so because for $N \leq 15$ the number of unknown parameters in the model exceeds the number of recorded samples. From Figure 6 many other interesting observations can be made. For instance, increasing N from 100 to 200, for a fixed K, is approximately equivalent to increasing the SNR with 3 dB. This holds in general: for $N \gg 1$, doubling the SNR gives the same effect as doubling N.

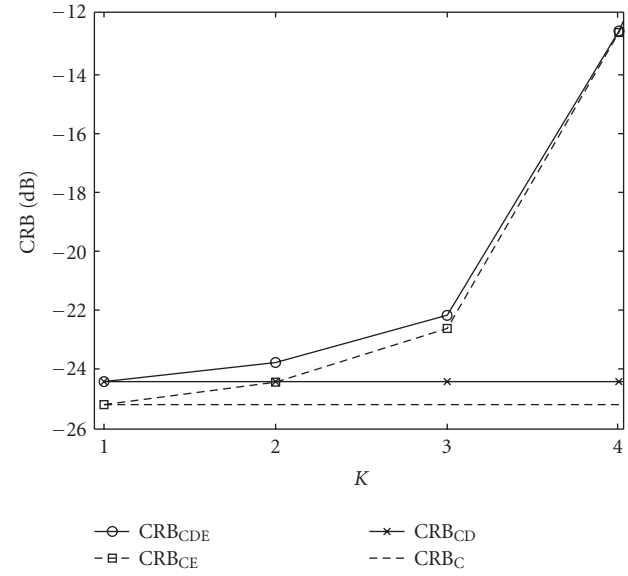

Figure 5: The CRB for the elements of $\mathbf{C}$ under different assumptions on whether $\mathbf{D}$, $\mathbf{E}$ are known or not, and for different K. SNR is 0 dB.

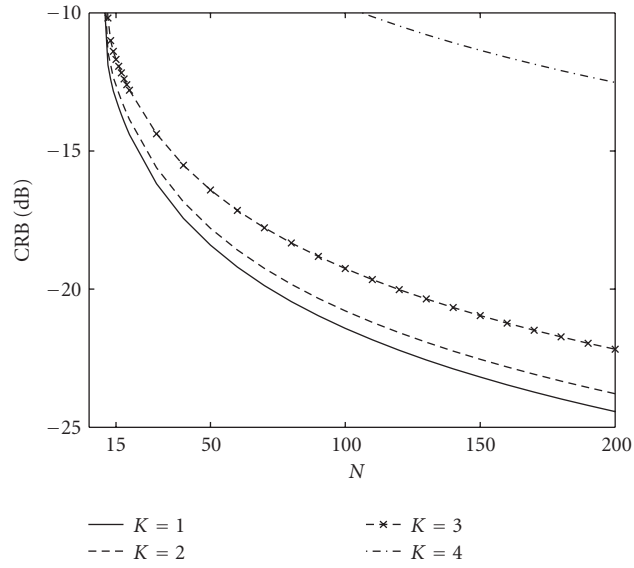

Figure 6: The CRB for the elements of $\mathbf{C}$ as a function of K and N when SNR is 0 dB.

5.3. Measured results on a dual polarized array

Next, let us study the performance of the proposed estimator on an actual antenna array. Data from an 8-column antenna array (see Figure 7) were collected at 1900 MHz during calibration measurements with 180 measurement points distributed evenly over the interval $\theta \in \{-90^\circ \cdots 90^\circ\}$. Uncompensated radiation patterns with mutual coupling are presented in Figure 8 for measured data of the array. The estimator presented in this paper was used to estimate the coupling matrix. The estimated coupling matrix was then used

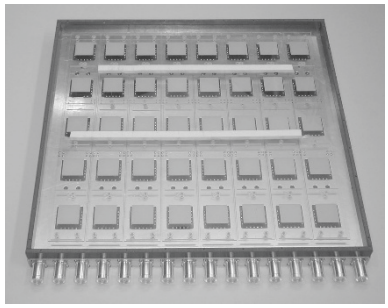

Figure 7: Eight-column dual polarized array developed by Powerwave Technologies Inc. Results are presented for this array in Section 5.3. Note that each vertical column of radiators forms an element with pattern $\widetilde{a}_m(\theta)$ in the horizontal plane.

to precompensate the data, after which radiation patterns can be obtained.

To modify our estimator (Section 3) to the dual polarized case, we follow [14]. Considering a dual polarized array with $\pm 45^\circ$ polarization and neglecting noise, (4) becomes

$$\begin{bmatrix} \mathbf{x}_{co}^{-45^\circ} & \mathbf{x}_{xp}^{-45^\circ} \\ \mathbf{x}_{xp}^{+45^\circ} & \mathbf{x}_{co}^{+45^\circ} \end{bmatrix} = \begin{bmatrix} \mathbf{C}_{11}\,\mathbf{ADE}_1 & \mathbf{C}_{12}\mathbf{ADE}_2 \\ \mathbf{C}_{21}\,\mathbf{ADE}_2 & \mathbf{C}_{22}\,\mathbf{ADE}_1 \end{bmatrix}, \tag{19}$$

where $\mathbf{x}_{co}^{-45^\circ}$ means measuring the incoming -45° polarized signal with the antenna elements of the same polarization, while $\mathbf{x}_{xp}^{-45^\circ}$ means the data measured at the -45° element when the incoming signal is $+45^\circ$. To estimate the total coupling matrix,

$$\mathbf{C}_{\text{tot}} = \begin{bmatrix} \mathbf{C}_{11} & \mathbf{C}_{12} \\ \mathbf{C}_{21} & \mathbf{C}_{22} \end{bmatrix}, \tag{20}$$

the four blocks of (19) are treated independently according to

$$\begin{aligned} \mathbf{x}_{co}^{-45^\circ} &= \mathbf{C}_{11}\mathbf{ADE}_1, & \mathbf{x}_{xp}^{-45^\circ} &= \mathbf{C}_{12}\mathbf{ADE}_2, \\ \mathbf{x}_{xp}^{+45^\circ} &= \mathbf{C}_{21}\mathbf{ADE}_2, & \mathbf{x}_{co}^{+45^\circ} &= \mathbf{C}_{22}\mathbf{ADE}_1. \end{aligned} \tag{21}$$

The $\mathbf{D}$ matrices of these four independent equations are equal. The E_1 matrix represents the copolarization blocks of (19), namely, $\mathbf{x}_{co}^{-45^\circ}$ and $\mathbf{x}_{co}^{+45^\circ}$, simultaneously and is modelled according to (5) with a set of $\boldsymbol{\alpha}$ parameters estimated by our method. For the cross-polarization, we assume isotropic element patterns, $\mathbf{E}_2 = \mathbf{I}$. Once the equations in (21) are solved, the total coupling matrix can be expressed using (20) and the radiation pattern of the measured data may be compensated by inverting the coupling matrix according to

$$\begin{bmatrix} \mathbf{x}_{\text{compensated}}^{-45^\circ} \\ \mathbf{x}_{\text{compensated}}^{+45^\circ} \end{bmatrix} = \mathbf{C}_{\text{tot}}^{-1} \begin{bmatrix} \mathbf{x}_{\text{measured}}^{-45^\circ} \\ \mathbf{x}_{\text{measured}}^{+45^\circ} \end{bmatrix}. \tag{22}$$

Figure 8(a) shows the individual radiation patterns of each antenna element as measured during calibration ($\mathbf{x}$). Figure 8(b) shows the radiation patterns after compensation by the coupling matrix ($C_{\text{iso}}^{-1}X$) when isotropic conditions are assumed by the estimator. This means assuming $\mathbf{E} = \mathbf{I}$, which is equivalent to setting $K = 1$ in our algorithm. The radiation patterns after compensation by the coupling matrix when using the proposed estimator with $K = 3$ are presented in Figure 8(c).

The results using an isotropic assumption on the element factor, Figure 8(b), shows an improvement over the uncompensated data of Figure 8(a). The graphs showing the copolarization (solid) are smoother and more equal to each other, which is what is expected from an array with equal elements when no coupling is present. The cross-polarization (dashed) is suppressed significantly compared to the uncompensated case. The estimated phase center is $\{\widehat{\delta}_x, \widehat{\delta}_y\} = [0.2\ 0]$.

Further improvement is achieved using our proposed method, Figure 8(c). Using $K = 3$, our method estimates the coefficients in the element factor representation (5) as $\widehat{\alpha} = [0.8\ \ -0.4\ \ 0.6]$ and the phase center as $\{\widehat{\delta}_x, \widehat{\delta}_y\} = [0.3\ \ 0]$. The resulting compensated radiation pattern of Figure 8(c) is even closer to the ideal array response when no coupling is assumed. The copolarization graphs are almost overlapping in the $\pm 60^\circ$ interval showing the radiation patterns of 8 equal elements with cosine-like element factors. The cross-polarization is also improved slightly over the isotropic case.

Phase diagrams representing the average phase error of the coupling matrix before and after compensation with the coupling matrix are presented in Figure 8(d). The phase error after compensation with $K = 3$ (Figure 8(d), bottom), modelling the phase shift and the element factor, is less than without the compensation (Figure 8(d), top). Assuming an isotropic element factor (Figure 8(d), middle) gives a better result than without compensation but not as good as the result of our method. This indicates that the validity of the estimated coupling matrix based on phase considerations increases with the proposed estimator. Furthermore, the results of our method with $K = 3$ show a notable improvement over the results presented in [14].

6. K-VALUE TRADEOFF BASED ON MONTE CARLO SIMULATIONS

We have seen in Section 5.2 that there is a tradeoff between K, N, and the SNR in terms of the CRB. In reality, the error in the estimation is a combination of both model- and noise-induced errors. Let us therefore study the overall performance of our proposed estimator using the root-mean-square error of the mutual coupling matrix:

$$\text{RMS} = \frac{1}{M^2}\|\mathbf{C} - \widehat{\mathbf{C}}\|_F = \frac{1}{M^2}\sqrt{\sum_{ij} |C_{ij} - \widehat{C}_{ij}|^2}, \tag{23}$$

where M^2 is the number of elements in $\mathbf{C}$. As an example, we use an 8-element linear array with spacing $d = \lambda/2$ and a true element factor given by $\boldsymbol{\alpha}_{\text{true}} = [0\,0\,1\,0\,\ldots]^T$. Simulations were conducted with our method for $K = 1 \ldots 5$ based on 1000 realizations and an SNR = 30 dB. The result is shown in Figure 9. The CRB for the given SNR level is also

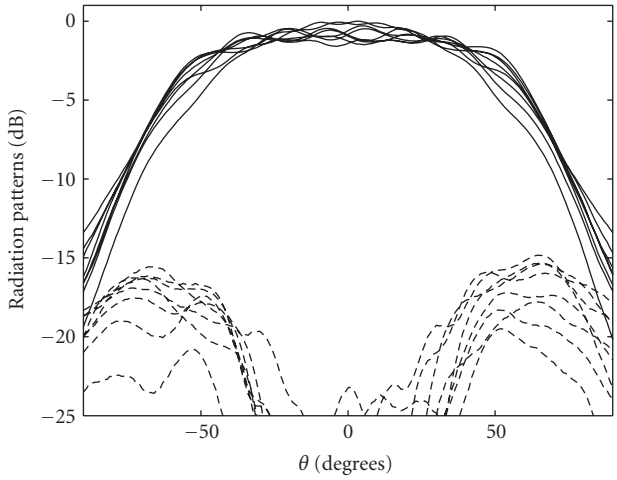

(a) Measured *uncompensated* radiation patterns for the array of Figure 7; $\{\mathbf{x}^{-45^\circ}_{\text{measured}}, \mathbf{x}^{+45^\circ}_{\text{measured}}\}^T$

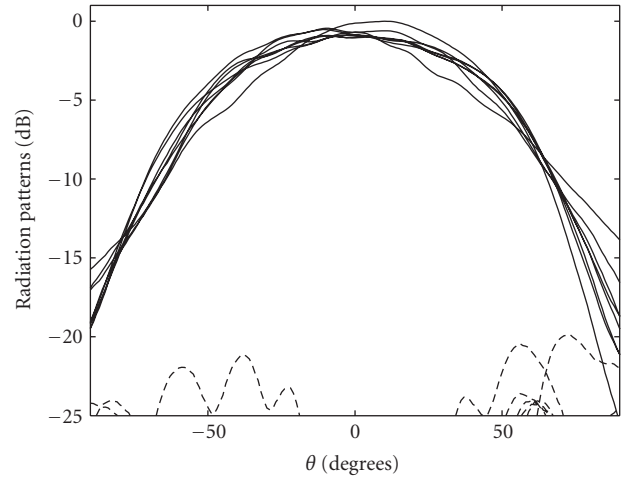

(b) Radiation patterns obtained from *compensated* data using a $\mathbf{C}$ matrix estimated via our algorithm setting $K = 1$ (i.e., forcing $\mathbf{E} \propto \mathbf{I}$); $\mathbf{C}^{-1}_{\text{iso}}\{\mathbf{x}^{-45^\circ}_{\text{measured}}, \mathbf{x}^{+45^\circ}_{\text{measured}}\}^T$

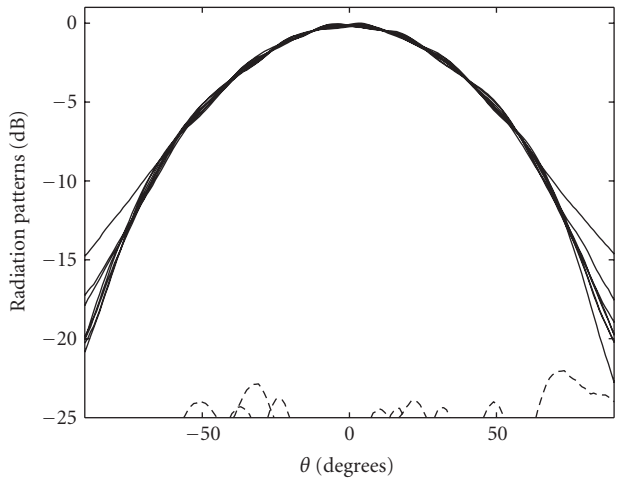

(c) *Compensated* radiation patterns using our method with $K = 3$; $\mathbf{C}^{-1}\{\mathbf{x}^{-45^\circ}_{\text{measured}}, \mathbf{x}^{+45^\circ}_{\text{measured}}\}^T$

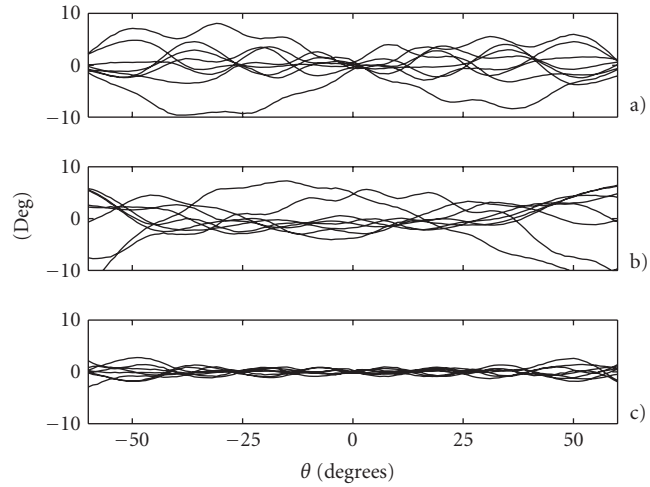

(d) Phase errors for the cases in (a), (b), and (c)

FIGURE 8: Radiation patterns obtained from compensated data with the coupling matrix $\mathbf{C}$ estimated in different ways. The measurements are from the 8-element dual polarized array in Figure 7 with co- (solid) and cross- (dashed) polarization collected during calibration.

presented in the same graph and represents the impact of the noise. This is seen as an increase of the CRB in the region $K > 3$.

Because of the insufficient parametrization of $\mathbf{E}$, the RMS is higher for smaller values of K than the true K. The RMS decreases toward the point where $K = 3$, which is the true value of K. For higher values of K, there is no longer a model error and the noise is the sole contributor to the RMS. This is evident as an increase in RMS when $K > 3$. The same estimation was also made with $\mathbf{E} = \cos^n\theta$ [13]. A straight line represents this case in Figure 9 showing the difference in RMS, which is higher compared to using our method with $K = 3$. This shows that the optimum tradeoff for our proposed method, in this case, is $K = 3$. This gives the best performance when comparing different values of K and the $\mathbf{E} = \cos^n\theta$ assumption.

7. CONCLUSIONS

We have introduced a new method for the estimation of the mutual coupling matrix of an antenna array. The main novelty over existing methods was that the array phase center and the element factors were introduced as unknowns in the data model, and treated as nuisance parameters in the estimation of the coupling as well, by being *jointly* estimated together with the coupling matrix.

In a simulated test case, our method outperformed the previously proposed estimator [13] for the case of an

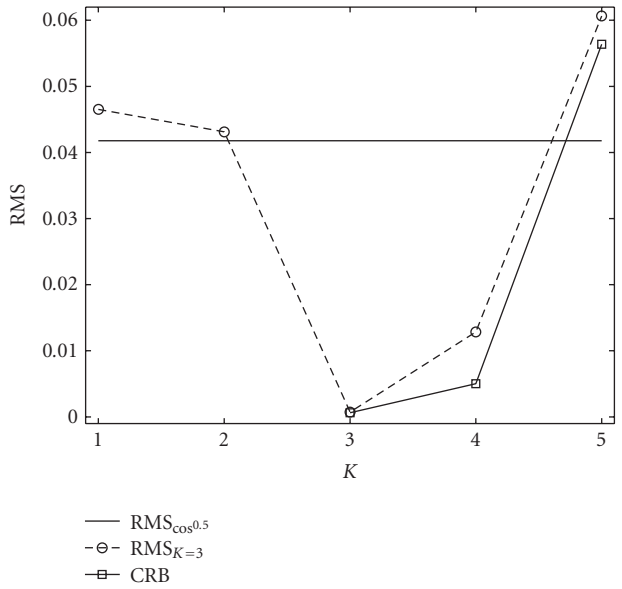

FIGURE 9: CRB and RMS based on Monte Carlo simulations when SNR is 30 dB. The true element factor is $\mathbf{E}_{\text{true}} = \cos 2\theta$, which means $\boldsymbol{\alpha}_{\text{true}} = [0\ 0\ 1\ 0\ 0]$ or $K_{\text{true}} = 3$.

8-element dipole array. The radiation pattern and phase error were significantly improved leading to increased accuracy in any following postprocessing.

Based on a CRB analysis, the SNR penalty associated with introducing a model for the element factor with two degrees of freedom ($K = 3$) was 2.5 dB relative to having zero degrees of freedom. This means that an additional 2.5 dB more power (or a doubling of the number of accumulated samples) must be used to retain the estimation accuracy of the coupling matrix compared to the case when the algorithm assumed omnidirectional elements. To add another degree of freedom (set $K = 4$) costs another 10 dB.

Using measured calibration data from a dual polarized array, we found that the proposed method and the associated estimator could significantly improve the quality of the estimated coupling matrix, and the result of subsequent compensation processing.

Finally, the tradeoff between the complexity of the proposed data model and the accuracy of the estimator was studied via Monte Carlo simulations. For the case of an 8-element linear array, the optimum was found to be at $K = 3$ which coincides with the true value in that case.

ACKNOWLEDGMENTS

This material was presented in part at ICASSP 2007 [19]. Erik G. Larsson is a Royal Swedish Academy of Sciences Research Fellow supported by a grant from the Knut and Alice Wallenberg Foundation.

REFERENCES

[1] D. Tse and P. Viswanath, *Fundamentals of Wireless Communication*, Cambridge University Press, Cambridge, UK, 2005.

[2] A. Swindlehurst and T. Kailath, "A performance analysis of subspace-based methods in the presence of model errors—part I: the MUSIC algorithm," *IEEE Transactions on Signal Processing*, vol. 40, no. 7, pp. 1758–1774, 1992.

[3] M. Jansson, A. Swindlehurst, and B. Ottersten, "Weighted subspace fitting for general array error models," *IEEE Transactions on Signal Processing*, vol. 46, no. 9, pp. 2484–2498, 1998.

[4] B. Friedlander and A. J. Weiss, "Effects of model errors on waveform estimation using the MUSIC algorithm," *IEEE Transactions on Signal Processing*, vol. 42, no. 1, pp. 147–155, 1994.

[5] H. Steyskal and J. S. Herd, "Mutual coupling compensation in small array antennas," *IEEE Transactions on Antennas and Propagation*, vol. 38, no. 12, pp. 1971–1975, 1990.

[6] J. Yang and A. L. Swindlehurst, "The effects of array calibration errors on DF-based signal copy performance," *IEEE Transactions on Signal Processing*, vol. 43, no. 11, pp. 2724–2732, 1995.

[7] C. A. Balanis, *Antenna Theory: Analysis and Design*, John Wiley & Sons, New York, NY, USA, 1997.

[8] T. Svantesson, "The effects of mutual coupling using a linear array of thin dipoles of finite length," in *Proceedings of the 9th IEEE SP Workshop on Statistical Signal and Array Processing (SSAP '98)*, pp. 232–235, Portland, Ore, USA, September 1998.

[9] K. R. Dandekar, H. Ling, and G. Xu, "Effect of mutual coupling on direction finding in smart antenna applications," *Electronics Letters*, vol. 36, no. 22, pp. 1889–1891, 2000.

[10] B. Friedlander and A. Weiss, "Direction finding in the presence of mutual coupling," *IEEE Transactions on Antennas and Propagation*, vol. 39, no. 3, pp. 273–284, 1991.

[11] T. Su, K. Dandekar, and H. Ling, "Simulation of mutual coupling effect in circular arrays for direction-finding applications," *Microwave and Optical Technology Letters*, vol. 26, no. 5, pp. 331–336, 2000.

[12] B. Lindmark, S. Lundgren, J. Sanford, and C. Beckman, "Dual-polarized array for signal-processing applications in wireless communications," *IEEE Transactions on Antennas and Propagation*, vol. 46, no. 6, pp. 758–763, 1998.

[13] M. Mowlér and B. Lindmark, "Estimation of coupling, element factor, and phase center of antenna arrays," in *Proceedings of IEEE Antennas and Propagation Society International Symposium*, vol. 4B, pp. 6–9, Washington, DC, USA, July 2005.

[14] B. Lindmark, "Comparison of mutual coupling compensation to dummy columns in adaptive antenna systems," *IEEE Transactions on Antennas and Propagation*, vol. 53, no. 4, pp. 1332–1336, 2005.

[15] S. M. Kay, *Fundamentals of Statistical Signal Processing: Estimation Theory*, Prentice-Hall, Upper Saddle River, NJ, USA, 1993.

[16] H. L. Van Trees, *Detection, Estimation, and Modulation Theory*, Wiley-Interscience, New York, NY, USA, 2007.

[17] J. Gorman and A. Hero, "Lower bounds for parametric estimation with constraints," *IEEE Transactions on Information Theory*, vol. 36, no. 6, pp. 1285–1301, 1990.

[18] P. Stoica and B. C. Ng, "On the Crameér-Rao bound under parametric constraints," *IEEE Signal Processing Letters*, vol. 5, no. 7, pp. 177–179, 1998.

[19] M. Mowlér, E. G. Larsson, B. Lindmark, and B. Ottersten, "Methods and bounds for antenna array coupling matrix estimation," in *Proceedings of IEEE International Conference on Acoustics, Speech, and Signal Processing (ICASSP '07)*, vol. 2, pp. 881–884, Honolulu, Hawaii, USA, April 2007.